Chapter

An Advanced Evapotranspiration Method and Application

Homin Kim and Jagath J. Kaluarachchi

Abstract

Estimating evapotranspiration is an important component in the monitoring of agricultural and environmental systems. This chapter will focus on the developing evapotranspiration method using general meteorological data and Normalized Difference Vegetation Index (NDVI). The proposed model in this chapter will be refined by using both the complementary relationship and the Budyko framework. The relative evaporation parameter in the complementary relationship will be derived by using precipitation, potential evapotranspiration, and NDVI based on that the Budyko framework can support the complementary relationship. It is also important to determine whether the proposed model can compete and deliver accuracy similar to remote sending method in the aspect of application. The results in the first phase showed the proposed model could be a powerful methodology to estimate ET among the ground-based method. In the second phase, a nonlinear correction function was proposed to better describe the complementary relationship. We will also demonstrate that the use of ET is a better approach for drought estimations than considering reference ET. More importantly, the advantage of the proposed model is that it can comprehensively consider both effects of precipitation and vegetation information. Taken together, this chapter has extended our knowledge of ET to support water resource management.

Keywords: evapotranspiration, complementary relationship, Budyko framework, Normalized Difference Vegetation Index (NDVI), drought monitoring

1. Introduction

Land surface evapotranspiration (ET) is an essential part of agricultural water management, and there are many classical methods including the Penman [1]. In the recent years, the Food and Agriculture Organization (FAO) version of Penman-Monteith Equation [2] is widely used to estimate ET. However, this method is limited for hydrologic purpose. For example, meteorological data need to be measured at 2-m elevation, and the FAO method is mainly used to estimate crop ET from agricultural lands using crop coefficients which are derived from unlimited water conditions and specific times of the growing cycle. As an alternative, the complementary relationship (CR) developed by Bouchet [3] can be used to estimate ET using general meteorological data. This approach proposed the first complementary function of potential evapotranspiration (ETP) and wet environment evapotranspiration (ETW) for a

wide range of available energy to estimate ET. Bouchet [3] postulated that the decrease in ET is matched by an equivalent increase in ETP as a surface dries. Later, Granger and Gray [4] model named as the GG model is one of the widely known models using the CR because it requires only meteorological data. Recently, Ref. [5] modified the GG model with meteorological data from 34 global eddy covariance sites. While the results were very good as compared other published ET methods, they mentioned that further refinements can improve performance under dry conditions. A probable reason is that the original GG model was empirically derived from wet biased environments in Canada. Taking this limitation into account, the model development was designed to extend the latest CR model using both meteorological data and NDVI. We then will validate the proposed model with other ET methods including a remote sensing model. Finally, we will address the possibility of using ET as a proxy for drought monitoring through a new drought index.

2. Development of complementary relationship model for estimating evapotranspiration

2.1 Introduction

ET is an important component in the climate system, and development of ET method has been studied by many researchers. As a result, there are many classical methods available for ET estimation based on data availability and required accuracy. One approach to estimate ET directly is the complementary relationship (CR) developed by [3]. Ref. [3] postulated that the decrease in evapotranspiration is matched by an equivalent increase in potential evapotranspiration (ETP) which is evaporation from a saturated surface, while energy and atmospheric conditions do not change. This idea has been widely tested in conjunction with the models of Priestley and Taylor [6] and Penman [1]. Among examples of widely known models, this study has focused on Granger and Gray [4] model because their model can directly estimate ET without the surface parameters or prior estimates of ETP. Furthermore, Ref. [5] extended the Granger and Gray [4] model to propose refinements to better predict regional ET especially under dry conditions and different land cover conditions. While the results of Anayah and Kaluarachchi [5] were very good, the authors also showed that further refinements can improve performance under dry conditions. In addressing the limitation of Anayah and Kaluarachchi [5] model which is named as the modified GG hereafter, this chapter is therefore to extend the modified GG model using a remote sending data, and this study is still committed to use minimal data such as meteorological data and other readily accessible information with no local calibration.

2.2 Methodology

In the CR developed by [3], ET is usually calculated by Eq. (1):

$$ET + ETP = 2ETW \tag{1}$$

where ETP is evaporation from a saturated surface and ETW is the value of potential evaporation when ET is equal to the potential rate. Based on the idea

of [3], Anayah and Kaluarachchi [5] developed their model using a three-step approach. First, they evaluated the original complementary methods under a variety of physical and climate conditions and developed 39 different model combinations. Second, three model variations were identified based on performance compared to observed data from a set of global sites. Third, a statistical analysis was conducted to contrast and compare the three models to identify the best (see detail in reference). Most importantly, the performance of the modified GG model increased by using the Priestley and Taylor [6] equation as shown in Eq. (2) to calculate EWT instead of the Penman [1] equation:

$$ETW = \alpha \frac{\Delta}{\gamma + \Delta}(R_n - G_{soil}) \tag{2}$$

where ETW is in mm/d, α is a coefficient equal to 1.28, R_n is net radiation in mm/d, γ is the psychrometric constant in kPa/°C, Δ is the rate of change of saturation vapor pressure with temperature kPa/°C, and G_{soil} is soil heat flux density in mm/d.

Also, there are two parameters: relative drying power (D) and relative evaporation (G). D and G are described in Eqs. (3) and (5), respectively:

$$D = \frac{E_a}{E_a + (Rn - G_{soil})} \tag{3}$$

where E_a is drying power of air in mm/d given in Eq. (4)

$$E_a = 0.35(1 + 0.54U)(e_s - e_a) \tag{4}$$

where U is wind speed at 2 m above ground level that needs adjustments and conducted using the procedure described by [2], e_s is saturation vapor pressure in mmHg, and e_a is vapor pressure of air in mmHg:

$$G = \frac{ET}{ETP} = \frac{1}{c_1 + c_2 e^{c_3 D}} \tag{5}$$

where c_1 is 1.0, c_2 is 0.028, and c_3 is 8.045. The effect of G_{soil} is negligible compared to R_n when calculated at monthly or higher time scale [7].

Solving Eq. (5) for ETP and substituting in Eq. (1), the modified GG model is given in Eq. (6):

$$ET = \frac{2G}{G + 1} ETW \tag{6}$$

Therefore, the modified GG model of Anayah and Kaluarachchi [5] can estimate ET directly without calculating ETP.

In the modified GG model, the ratio of ET to ETP is defined as relative evaporation, G, as shown in Eq. (5), and parameter G was empirically derived using limited data from wet environments in Western Canada [4]. This bias towards wet region data may be the reason for relatively poor estimations with the modified GG model under dry conditions. In order to improve the ET predictions of the modified GG model, parameter G needs improvement. For this purpose, we use the theoretical framework of Budyko [8] on the basis of that the CR is consistent with the Budyko

hypothesis through the Fu equation [9, 10]. The analytical solution of the Budyko framework is given in Eq. (7):

$$\frac{ET}{ETP} = 1 + \frac{P}{ETP} - \left[1 + \left(\frac{P}{ETP}\right)^{\omega}\right]^{1/\omega} \tag{7}$$

where P is precipitation in mm and ETP is estimated using the Priestly and Taylor equation [6]. Parameter ω is constant and represents the land surface conditions, especially the vegetation cover [11]. Parameter ω is linearly correlated with the long-term average annual vegetation cover, and a model using NDVI can improve the estimation of ET (see details in [5]). Thus, Eq. (8) shows the Fu equation where parameter G is now defined as G_{new}:

$$G_{new} = \frac{ET}{ETP} = 1 + \frac{P}{ETP} - \left[1 + \left(\frac{P}{ETP}\right)^{\omega}\right]^{1/\omega} \tag{8}$$

Note G_{new} in Eq. (8) is required and can be estimated using the Penman [1] given in Eq. (9):

$$ETP = \frac{\Delta}{\Delta + \gamma}(R_n - G_{soil}) + \frac{\gamma}{\gamma + \Delta}E_a \tag{9}$$

Having found G_{new} from Eq. (8) and estimating ETW from Eq. (2), we can estimate ET from Eq. (10):

$$ET = \frac{2G_{new}}{G_{new} + 1}ETW \tag{10}$$

Hereafter, this proposed model will be referred as the GG-NDVI model. This chapter used two phases to evaluate the performance of the proposed model. In phase 1, the GG-NDVI model compared with two CR models: the complementary relationship areal evapotranspiration (CRAE) model of [12] and the modified GG model of [5]. Moreover, comparisons are made between a commonly used remote sensing model and GG-NDVI model. In phase 2, a comparison of estimated ET from GG-NDVI with observed data from phase 1 will be performed to identify the weaknesses of the CR model, and appropriate corrections will be proposed.

2.3 Data

ET estimation from GG-NDVI was generated using meteorological data and NDVI. Meteorological data required are temperature, wind speed, precipitation, net radiation, and elevation (pressure). Among these, net radiation (R_n) was calculated using the equations by [2]. This chapter proposes to use data from AmeriFlux eddy covariance sites in the United States because the US sites have wide variety of climate and physical conditions and land cover especially in dry regions. In phase 1, although we selected 75 sites of Level 2 data of AmeriFlux with fewer than 50% missing data and these data were obtained from the Oak Ridge National Laboratory's website (http://ameriflux.ornl.gov/), we used only 59 sites since only these sites have incident global radiation data required by the

CRAE model. After we validated GG-NDVI with ground-based ET models, we also compared with a remote sensing model. Air temperature, elevation, and precipitation data were obtained from the Parameter-elevation Regressions on Independent Slopes Model (PRISM, http://www.prism.oregonstate.edu). As part of the input data for the GG-NDVI model, we used the 16-day NDVI data from MODIS (http://daac.ornl.gov/MODIS/modis.shtml). We also collected the lever 4 meteorological data including latent heat flux (LE) from 76 AmeriFlux stations, and then we excluded those stations with actual vegetation type different from the MODIS global land cover product (MOD12) at any of surrounding 500 m by 500 m spatial resolution. Also, we further excluded those stations with fewer than half a year of measurements during 2000–2007. As a result, 60 AmeriFlux stations were used in the comparison of the remote sending model as shown in **Figure 1**.

We defined the climate class of each site using the aridity index of the United Nations Environment Programme (UNEP) proposed by [13]. The aridity index divided climate conditions to six classes: hyper-arid, arid, semiarid, dry subhumid, wet subhumid, and humid. However, this work simplified the climate class definition to two classes, dry and wet.

2.4 Results

2.4.1 Phase 1: validation

The CRAE model is considered as a simple, practical, and reliable model to estimate monthly ET [7]. The modified GG model had been validated by [5] that it showed better performance compared to the recently published works. Therefore, the phase 1 provides the opportunity to test both models compared to the proposed GG-NDVI model. The results of the comparison are given in **Table 1** and **Figure 2**. The GG-NDVI model showed the lowest mean RMSE across all models about 15 mm/month in dry sites and about 12 mm/month in wet sites. The results in general indicate that GG-NDVI can perform well in the dry conditions and even better

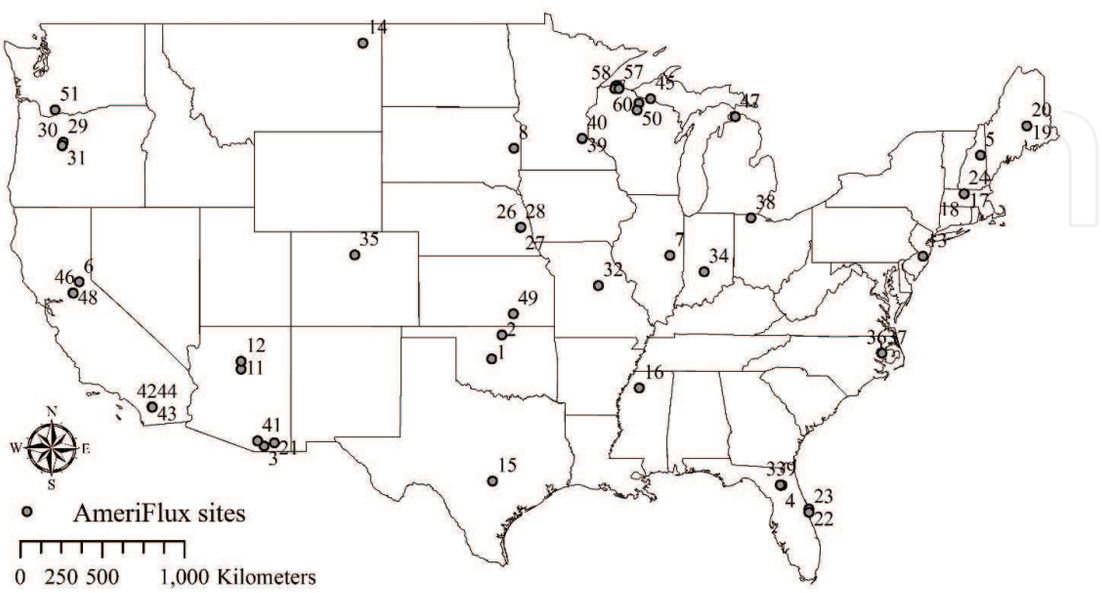

Figure 1.
Locations of 60 AmeriFlux sites used in phase 2 with number.

	29 dry sites			30 wet sites		
	Min	Mean	Max	Min	Mean	Max
Modified GG	1.7	21.4	42.7	0.6	12.9	36.0
GG-NDVI	0.4	14.7	56.6	0.3	11.6	28.5
CRAE	0.5	18.9	53.9	0.8	22.3	62.3

Table 1.
Comparison of RMSE (mm/month) between different complementary relationship models.

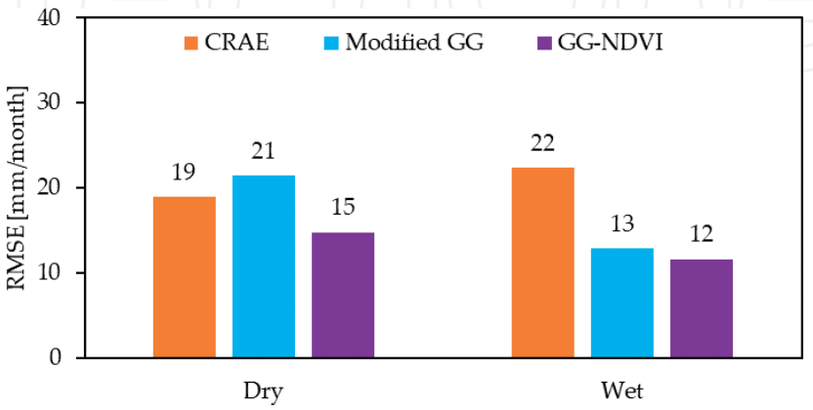

Figure 2.
Comparison of RMSE (mm/month) between different complementary relationship models for 29 dry and 30 wet sites in the United States [15].

in the wet conditions. These results also confirm that the estimation capability of ET reduces with increased aridity [5, 7, 14].

Overall, these results indicate that, among the ground-based methods, the GG-NDVI model can be used as a powerful methodology to estimate ET (see [15]).

While these findings are good within the realm of CR methods, some of the more commonly used ET estimation model now use remote sensing data. Therefore, we selected the operational Simplified Surface Energy Balance (SSEBop), which is one of the widely used remote sensing model developed by [16], and SSEBop can be easily retrieved from the USGS Geo Data Portal (http://cida.usgs.gov/gdp/). **Table 2** presents the yearly comparison of results between the SSEBop and GG-NDVI estimates. Compared with measured ET, the results indicate that the accuracy of SSEBop and GG-NDVI estimates show satisfactory R-square and RMSE values. R-square values for SSEBop and GG-NDVI are 0.65 and 0.61, respectively. The results demonstrate that the ET estimates from GG-NDVI ET at an annual time scale are reasonable.

According to **Table 2** and **Figure 3**, the mean RMSE of GG-NDVI ranged between 15 and 20, and GG-NDVI showed lower RMSE than SSEBop every year from 2000 to 2007. Although the magnitude of agreement (overestimation or underestimation) seems to vary from site to site and from season to season, **Figure 3** confirms that the occurrence of an RMSE less than 20 mm/month with GG-NDVI is more frequent than with SSEBop in both dry and wet sites. The mean RMSE across 24 dry sites for GG-NDVI and SSEBop is 19 and 22 mm/month, respectively.

Based on these results, we could conclude that GG-NDVI is a reliable approach for estimating ET showing a reasonable match with measured ET of AmeriFlux sites. However, GG-NDVI may not predict ET accurately when the vegetation cover

Year	AmeriFlux mean [mm/month]	R-square		RMSE [mm/month]	
		SSEBop	GG-NDVI	SSEBop	GG-NDVI
2000	43	0.82	0.79	16	15
2001	44	0.54	0.58	23	20
2002	41	0.73	0.67	19	16
2003	42	0.68	0.65	21	17
2004	42	0.68	0.60	18	18
2005	42	0.37	0.57	28	18
2006	41	0.61	0.55	20	18
2007	34	0.40	0.40	18	17
All years	44	0.65	0.61	19	18

Table 2.
Comparison of monthly ET estimates between SSEBop and GG-NDVI using AmeriFlux data from 2000 to 2007.

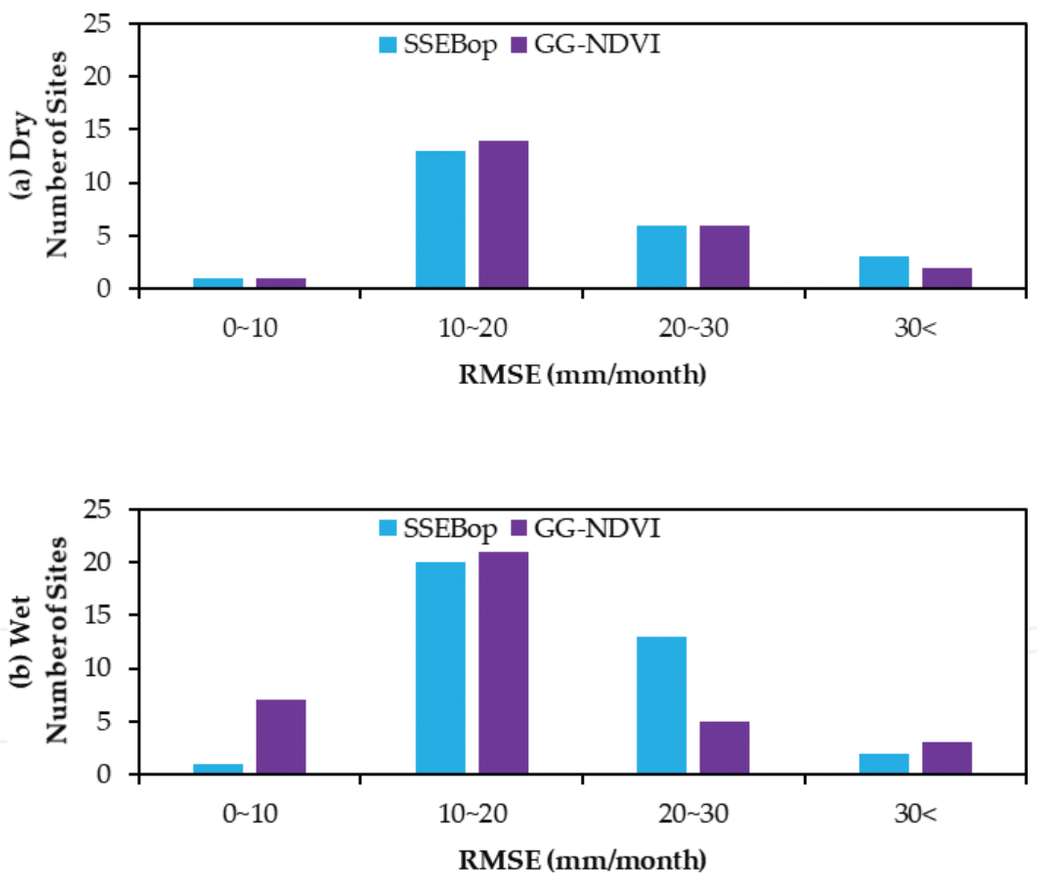

Figure 3.
Histogram of RMSE (mm/month) of SSEBop and GG-NDVI for (a) 24 dry and (b) 36 wet sites.

changes significantly or is dense. A possible reason is that the relationship between NDVI and vegetation can be based where a Leaf Area Index (LAI) is less than 3. According to [7], a Soil-Adjusted Vegetation Index (SAVI) is recommended instead of NDVI when the LAI is less than 3. Thus, the limitations of NDVI to represent vegetation under specific conditions may be the reason for the decreased performance of GG-NDVI.

2.4.2 Phase 2: enhancement of GG-NDVI

GG-NDVI increases the predictive power with increasing humidity similar to other CR models. One interesting finding is the RMSE of GG-NDVI increases slightly with the relative evaporation, parameter G, as shown in **Figure 4**. Considering this observation, phase 2 focused on the relationship between the performance of GG-NDVI and parameter G. Within the complementary relationship, increasing G means that climate is becoming wetter and ET is closer to ETW. When ET equals to ETW, surface has access to unlimited water as shown in **Figure 5**. However, natural surfaces in even the wettest regions may not approach complete saturation. Consequently, the magnitude of difference between ET and ETW is important in estimating ET. A possible explanation could be that the CR between ET and ETP is not symmetric. GG-NDVI has improved the performance of the Granger and Gray [4], but Eq. (10) still contains the value of two meaning of a symmetric complementary relationship as first developed by [3]. Furthermore, other studies question the use of the symmetric relationship [15, 17, 18]. Taking this into account, a correction function as a function of G is proposed as shown in **Figure 5** and Eq. (11):

$$ET = \frac{2Gnew}{Gnew + 1} \times f(G) \times ETW \tag{11}$$

We expect the correction function to be nonlinear, similar to an exponential function, since the magnitude of the difference between ET and ETP decreases exponentially. The correction function can be calculated by Eq. (12), and we fitted 2772 data points to compute the values of α and β coefficients:

$$f(G) = \alpha \exp^{\beta \cdot G} \tag{12}$$

Regression analysis found α is 0.7895 and β is 0.9655. Hereafter, the GG model with the correction function given as Eq. (11) is called the Adjusted GG-NDVI model.

To evaluate the performance of Adjusted GG-NDVI, we compared the monthly ET estimations with SSEBop across 60 sites. **Figure 6** presents a histogram of RMSE from three models and shows a significant improvement attributed to the Adjusted GG-NDVI model. With the correction function, 38 sites have less than 15 mm/month of RMSE, compared to 26 sites with GG-NDVI and 20 sites with SSEBop. The results demonstrate that the use of the correction function can significantly improve accuracy in estimation ET. In addition, Eq. (11) can be updated with the new definition of G as

$$ET + ETP = 2f(G)ETW \tag{13}$$

The new formulation of the Adjusted GG-NDVI model described in Eq. (13) clearly shows that the relationship between ET and ETP is not symmetric with respect to ETW, further confirming the earlier conclusions that the idea of [3] needs to be extended and applied with appropriate corrections.

With an advanced ET model, we address the possibility of using ET as a proxy for drought monitoring through a new and reliable drought index than using potential evaporation in the next chapter.

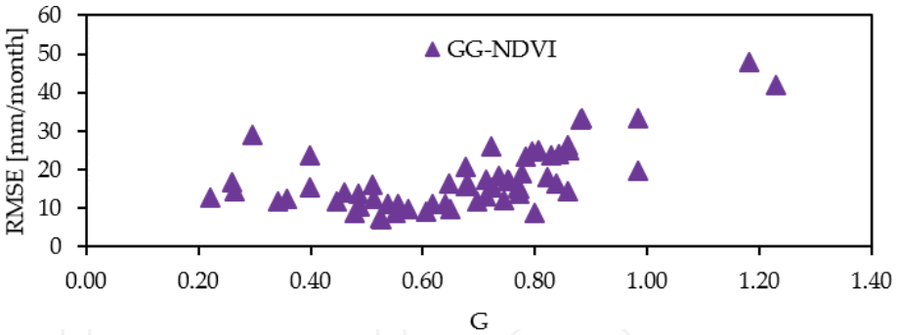

Figure 4.
RMSE of GG-NDVI versus the relative evaporation, parameter G (ET/ETP).

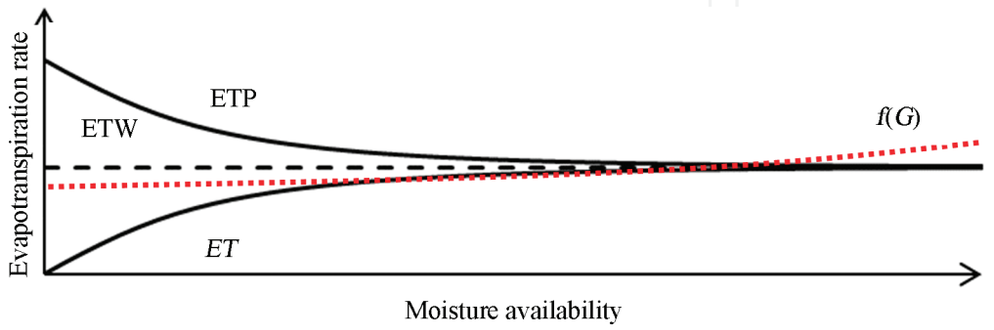

Figure 5.
A schematic representation of the complementary relationship between ET, ETP, and ETW with the proposed correction function, f(G).

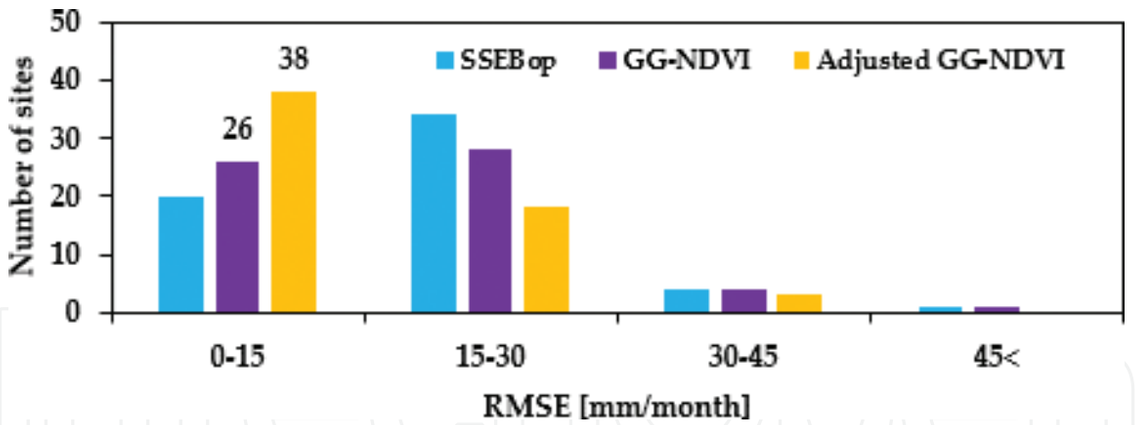

Figure 6.
Comparison of RMSE between different ET models.

3. Application of the evapotranspiration model in drought monitoring

3.1 Introduction

Many operational drought indices focus on the effects of precipitation and temperature for drought monitoring, and the state-of-the-art drought monitoring indices were developed to address vegetation condition with advanced remote sensing technology. However, only a few are focused on the use of actual ET when a drought index is defined. The Standardized Evapotranspiration Deficit Index

(SEDI, [19]) was developed by using actual ET based on [3] and a structure of the SPI. They estimated ET using the modified GG model of Anayah and Kaluarachchi [5] and ETW minus ET to measure drought conditions. As a result, the spatial patterns of the SEDI were consistent with the PDSI and SPI over the contiguous United States (CONUS), and this index could roughly identify vegetative droughts such as a Vegetation Health Index (VHI). Although the results of SEDI demonstrated that the use of actual ET can provide a reliable measure for drought monitor, it would have been much more useful if the authors addressed the precipitation and used the accurate ET model. Taking these limitations into account, this chapter has focused on developing a drought index with an advanced ET model including precipitation and remote sending vegetation information. The specific object is to evaluate the applicability of the proposed drought index over the CONUS by comparing it with US Drought Monitor (USDM) which is most widely used tool in the United States.

3.2 Methodology

We propose to develop a simple drought index called the evapotranspiration Water Deficit Drought Index (EWDI), which is derived from precipitation, meteorological data, and vegetation information. EWDI uses the structure of SPI with the monthly difference between ETW and ET. This value represents water deficit using the complementary relationship. The complementary relationship to estimate ET was addressed in the previous sections and a nonparametric approach to calculating the probability-based drought index will be addressed in this sector.

3.2.1 EWDI formulation

With a known ET value, the difference between ETW and ET for the month i is calculating using Eq. (14):

$$D_i = ETW_i - ET_i \tag{14}$$

Given the monthly time series of D_i, EWDI uses a nonparametric approach in which empirically derived probabilities are obtained through an inverse normal approximation [20] because this probabilities approach allows a consistent comparison between EWDI against other standardized indices [21, 22].

The probability distribution function of the D_i, according to the Tukey distribution, is given by Eq. (15):

$$P(D_i) = \frac{i - 0.33}{n + 0.33} \tag{15}$$

where $P(D_i)$ is the empirical probability of D_i which is aggregated across the period of interest. In this study, we used 12-month duration for accumulating D_i because 9- to 12-month time scale is the most useful in estimating the extreme drought conditions [23]. For example, to calculate a 12-month EWDI in December, D_i is summed over the period from January to December. i is the rank of the aggregated D_i in the historical time series ($i = 1$ is the maximum D_i), and n is the number of observations in the series being ranked. EWDI then can be easily derived following the classical approximation of [20] as shown in Eq. (16):

$$EWDI = W - \frac{C_0 + C_1 W + C_2 W^2}{1 + d_1 W + d_2 W^2 + d_3 W^3} \tag{16}$$

where

$$W = \sqrt{-2\ln P(D_i)} \text{ for } P(D_i) \leq 0.5 \quad (17)$$

If $P(D_i) > 0.5$, replace $P(D_i)$ with $[1 - P(D_i)]$ and the sign of EWDI is reversed. The constants are $C_0 = 2.515517$, $C_1 = 0.802853$, $C_2 = 0.010328$, $d_1 = 1.432788$, $d_2 = 0.189269$, and $d_3 = 0.001308$. The average value of EWDI is 0, and the standard deviation is 1. A zero EWDI means that D_i accumulated over the aggregation period in the year of interest is equal to the median value, positive value indicates drought, and negative is wet condition.

Hereafter, drought index EWDI estimated from the modified GG [5] is called EWDI-MOD. Similarly, drought index EWDI estimated from GG-NDVI [24] is called EWDI-NDVI.

3.3 Data

Required meteorological data to calculate both ET values (modified GG or GG-NDVI) are air temperature, precipitation, elevation (pressure), net radiation, wind speed, and NDVI. Net radiation was estimated using the equations suggested by [25]. Air temperature and precipitation data are from the PRISM (Parameter-elevation Regressions on Independent Slopes Model) climate group (available at http://prism.oregonstate.edu/) at 4-km resolution for the period 2000–2015 covering the CONUS. Wind speed was collected from the Climate Monitoring at NOAA's National Centers for Environmental Information (available at https://www.ncdc.noaa.gov/societal-impacts/wind/). Monthly NDVI data required for the GG-NDVI method are from the NASA Earth Observations (NEO, available at http://neo.sci.gsfc.nasa.gov/).

To assess the capability of EWDI, we used USDM to compare the differences between the two indices during the evolution of drought through time and space. USDM is derived from measurements of climatic, hydrologic, soil conditions, and regional expert comments [26]. USDM is not a forecast instead it assesses the current drought conditions. USDM divides drought severity into five classes: abnormally dry (D0), moderate drought (D1), severe drought (D2), extreme drought (D3), and exceptional drought (D4). All drought indices used in this study were converted to USDM classes as presented in **Table 3**. Additionally, we compared EWDI against PDSI and SPI which were retrieved from the WestWide Drought Tracker (WWDT, available at http://www.wrcc.dri.edu/wwdt/about.html). USDM data from 2000 to 2015 were collected from the USDM website (http://

Drought condition	USDM	PSDI	SPI	EWDI
Abnormally dry	D0	−1.0	−0.5	−0.5
Moderate drought	D1	−2.0	−0.8	−0.8
Severe drought	D2	−3.0	−1.3	−1.3
Extreme drought	D3	−4.0	−1.6	−1.6
Exceptional drought	D4	−5.0 >	−2.0 >	−2.0 >

All indices data from 2001 to 2015 were collected.

Table 3.
Drought classes of USDM and corresponding threshold value for classifying drought with PDSI, SPI, and EWDI.

droughtmonitor.unl.edu/Home.aspx), and four indices are resampled to match the 4-km resolution of EWDI using bilinear interpolation in the ArcMap software.

We also used EC flux tower data (in mm/month) from FLUXNET stations to perform a comparison of modified GG and GG-NDVI ET products. The latent heat flux data were collected from the Oak Ridge National Laboratory's AmeriFlux website (http://ameriflux.ornl.gov/, last accessed on November 23, 2016). The tower-measured monthly latent heat flux data were calculated using the equation as $ET = LE/\lambda$, where LE is the latent heat flux (W/m^2) and λ is the latent heat of vaporization (2.45 MJ/kg).

3.4 Results

The Pearson correlation coefficient was used to determine which ET method is the best estimating drought. Like SPI and other drought indices, EWDI can be estimated at different time scales from which specific time aggregated versions are selected. **Figure 7** provides the results obtained from the correlation coefficient between two EWDI results and USDM for years 2001–2015. EWDI using the GG-NDVI ET model generally shows a stronger relationship with UDSM across CONUS. The area-averaged correlation coefficient over all pixels for EWDI-MOD is 0.58, whereas EWDI-NDVI produced 0.72. Also, correlations between EWDI-NDVI and USDM are strongest over much of the southern and northern rockies and plains of the US climate regions and highest in Texas ($r > 0.8$). This observation is consistent with the regions where soil moisture on land surfaces makes the largest contributions to ET, referred as "hot spot" of land-atmosphere coupling by [27]. It can be clearly seen from **Figure 7** that a significant improvement is attributed to the GG-NDVI model in northwest, upper midwest, and northeast climate regions of the United States. Moreover, the improved performance of EWDI-NDVI over the CONUS can be seen from **Figure 8**. The drought conditions of EWDI-NDVI are similar to that estimated by USDM as shown in **Figure 8(a)**. Also, EWDI-NDVI produced extreme drought conditions much better than EWDI-MOD as shown in **Figure 8(b)**. It is very much plausible that these improved results are due to the use of an accurate ET model.

To further study these results, the San Bernardino County in California was selected as shown in **Figure 9**. The area-averaged correlation coefficient over all pixels in California is 0.55 for EWDI-MOD and 0.70 for EWDI-NDVI. The EWDI-MOD showed lower correlation (0.4–0.6) for most of San Bernardino County, and even the northern county values ($r < 0.2$) were much lower than the county

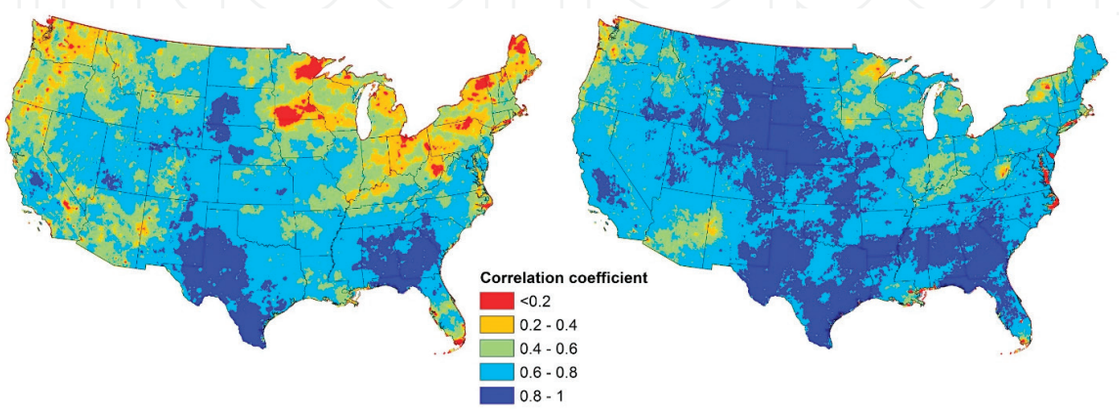

Figure 7.
Correlation coefficient between two EWDIs and USDM. EWDI-MOD (left) represents EWDI using the modified GG [5], and EWDI-NDVI (right) represents EWDI using GG-NDVI [15]. The area-averaged correlation coefficient over all pixels for EWDI-MOD and EWDI-NDVI is 0.58 and 0.72, respectively.

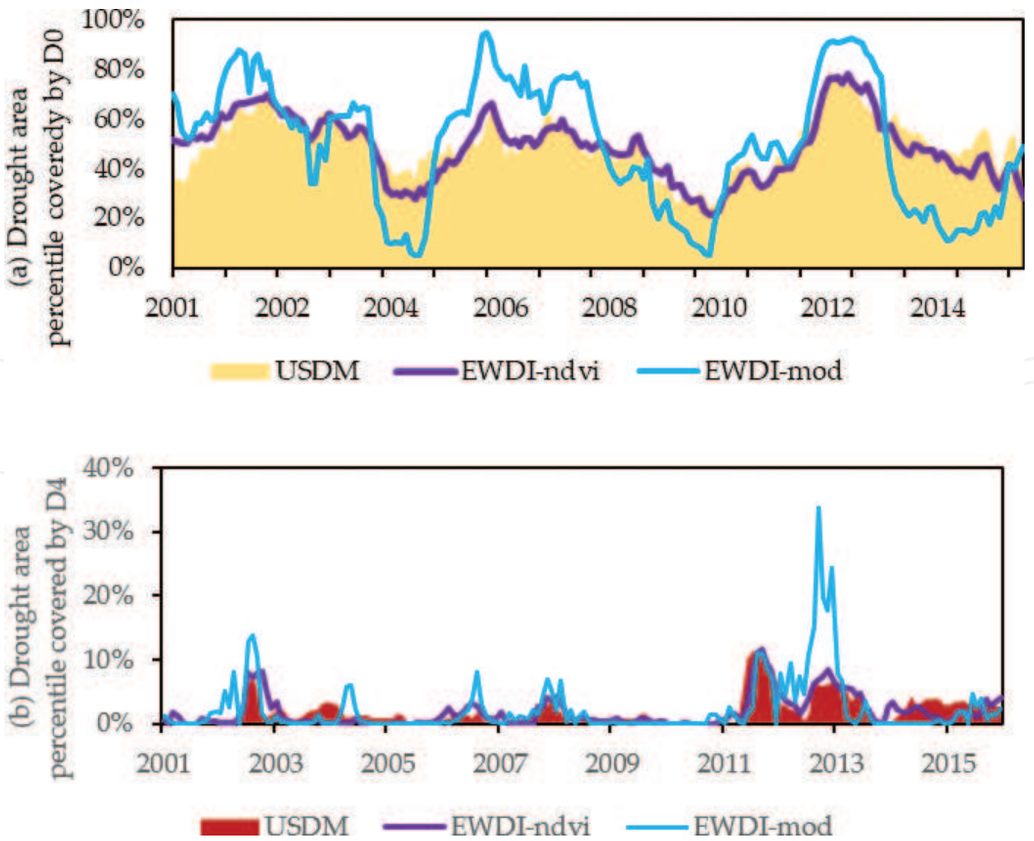

Figure 8.
Percent area of CONUS (a) covered by D0 (abnormally dry) and (b) covered by D4 (exceptional drought) from 2001 to 2015.

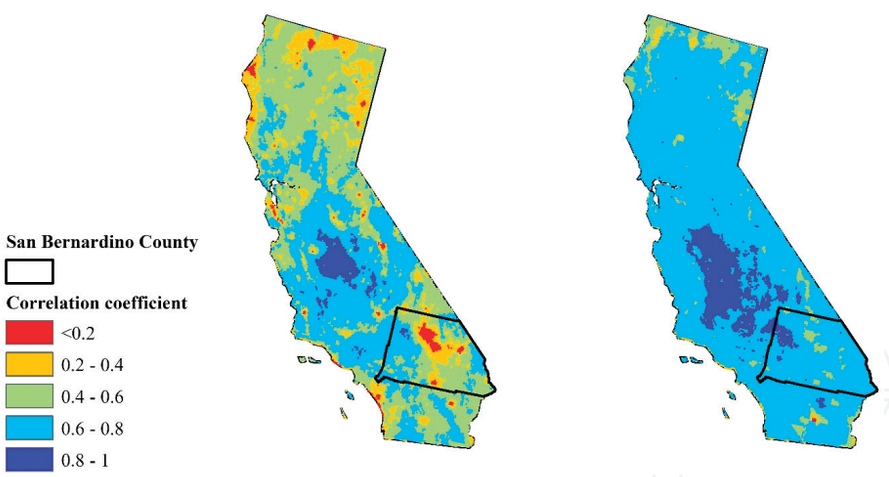

Figure 9.
Correlation coefficient for EWDI-MOD (left) and EWDI-NDVI (right) for California and San Bernardino County (black line).

area-averaged correlation coefficient of 0.51. However, the correlation coefficients of EWDI-NDVI were between 0.6 and 0.8 for most of California, and the county area-averaged values increased by 40% compared to EWDI-MOD.

To compare the temporal drought patterns of EWDI-MOD and EWDI-NDVI, **Figure 10** presents percent area of San Bernardino County covered by D0 from 2012 to 2015. This time period was selected because observed ET data are only available from 2012 to 2015. As shown in **Figure 10(a)**, both produced similar drought conditions until the middle of 2012. Thereafter, EWDI-MOD overestimated drought until May 2013 and underestimated compared to USDM in 2014 and 2015. It is therefore

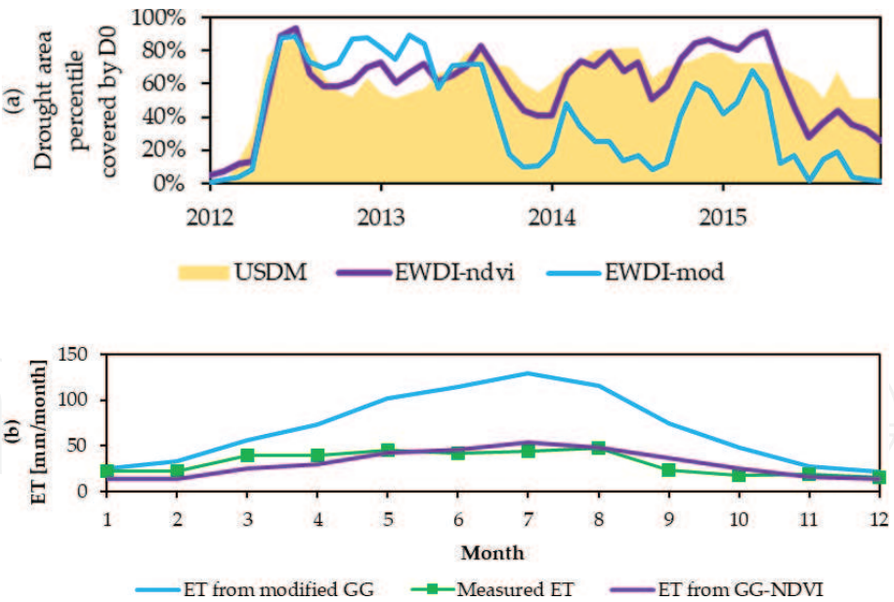

Figure 10.
(a) Percent area of San Bernardino County covered by D0 and (b) monthly estimated ET values from the modified GG and GG-NDVI models and mean monthly observed ET from 2012 to 2015.

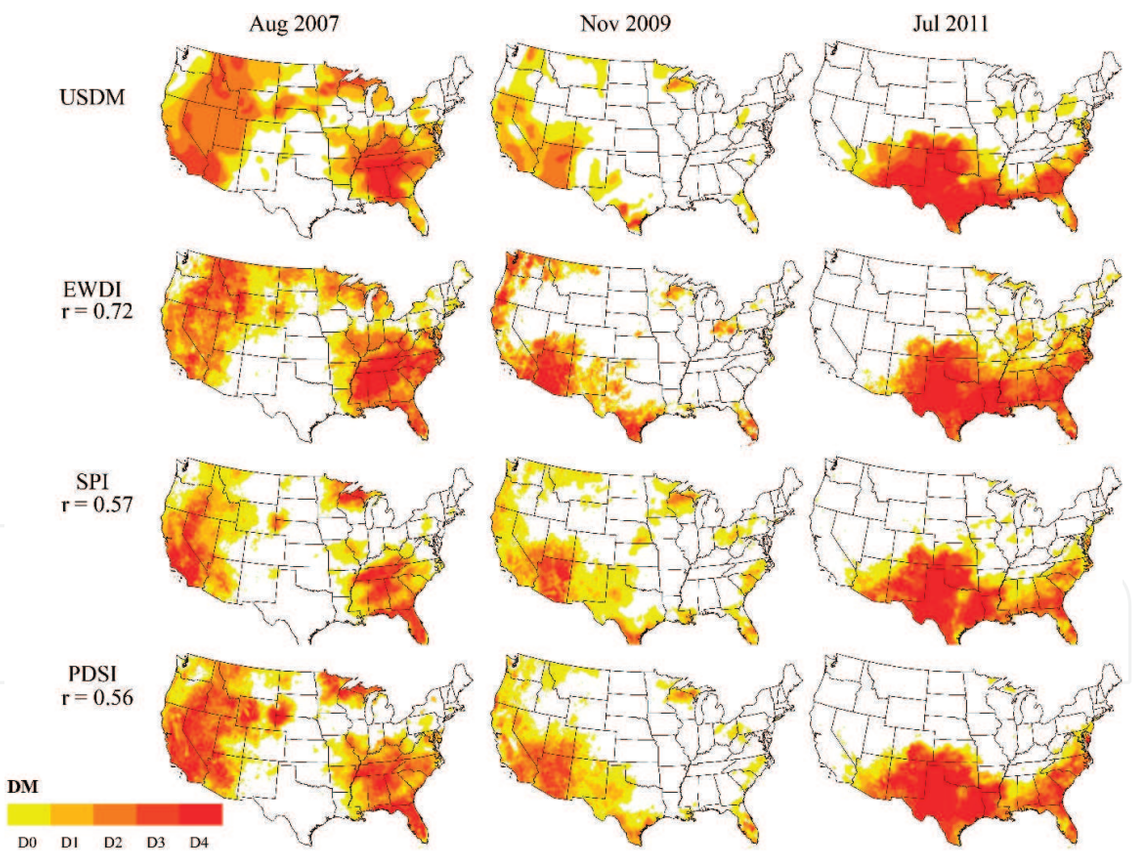

Figure 11.
Spatial distributions of USDM, EWDI, SPI, and PDSI results for major drought months in the CONUS. The quantity of r shown in figure means the correlation coefficient with USDM from 2001 to 2015.

possible to state that EWDI-NDVI estimated the drought condition better than EWDI-MOD. These results may be explained by comparing ET values shown in **Figure 10(b)**. The plot shows GG-NDVI ET against observed ET and the same with the modified GG estimates from 2012 to 2015. The results show that the pattern of ET from modified GG is much higher than observed ET, whereas GG-NDVI shows similar patterns with observed ET. The mean RMSE is 37 mm/month for modified

GG and 7 mm/month for GG-NDVI. The overestimated ET from modified GG, which brings a small water deficit, results in a corresponding drought that is underestimated compared to USDM. Taken together, these results indicate that the water deficit derived from the complementary relationship can be used as a drought index and the use of an accurate ET method can improve the performance of EWDI (**Figure 11**).

4. Summary and conclusions

This study proposed an improved version of the Granger and Gray [4] using both the complementary relationship and the Budyko framework in Chapter 2. Then, existing limitation of the complementary relationship was identified by comparing remote sensing ET product. Lastly, the applicability of using accurate ET model as a drought index was addressed in Chapter 3.

In Chapter 2, the modified GG model developed by [5] was refined by using the Budyko framework based on [11]. The relative evaporation parameter in the original GG model was derived from limited sites under wet conditions in Canada [4]. To overcome this limitation, the Fu equation [11] was used instead of the relative evaporation parameter on the basis that the Fu equation can support the complementary relationship [9, 10]. This chapter used AmeriFlux eddy covariance tower sites in the United States to retrieve required meteorological data including precipitation. Also, NDVI were from the MODIS land subsets. Sites were divided into dry and wet climate conditions based on an aridity index from UNEP [13]. The proposed model, denoted as GG-NDVI, showed much lower RMSE in both dry and wet sites compared to the modified GG model (see details in [5]). More importantly, the validation in Chapter 2 provided an inherent limitation of the complementary relationship and validation through a direct comparison with the SSEBop (Operational Simplified Surface Energy Balance, [16]). The SSEBop ET data set retrieved from the USGS Geo Data Portal for the period 2000–2007 covering the United States and 60 AmeriFlux stations were used for validation of ET results from SSEBop and GG-NDVI. The results showed that GG-NDVI can produce similar or better accuracy than SSEBop. Based on the results, this study observed that the assumption of symmetric complementary relationship was a deficiency in GG-NDVI that produced poor results under certain condition. Under the symmetric complementary relationship, ET is close to ETW with increasing humidity, but natural surfaces even in the wettest regions will not approach saturation. Therefore, this study proposed a nonlinear correction function to the GG-NDVI to better describe the complementary relationship. This correction function improved the GG-NDVI model significantly especially, under conditions of high humidity and dense vegetation.

In Chapter 3, ET calculated from the latest version of GG-NDVI, denoted as Adjusted GG-NDVI, used to estimate drought conditions across the United States for the period of 2001–2015. The proposed drought index, EWDI, was calculated by using the difference between ETW and ET with the probability distribution function of [20] because this probabilistic approach allowed a consistent comparison between EWDI and other standardized indices. Also, the drought severity of EWDI was divided into five classes that are the same classes with the US Drought Monitor (USDM). Required meteorological data were from the PRISM at 4-km resolution covering the CONUS, and monthly NDVI data were retrieved from the NASA Earth Observations. The results of this chapter supported that the EWDI could capture drought conditions and using an accurate ET model can help to improve drought monitoring performance. One unanticipated finding was that within the complementary relationship when energy-limited conditions are present, ET and ETW

varied in a parallel trend and ET is closer to ETW, resulting in decreasing EWDI performances such as Minnesota (not shown in this study). Despite this limitation, EWDI could identify droughts over CONUS consistent with USDM from the major drought incidents of August 2007, November 2009, and July 2011.

Author details

Homin Kim[1*] and Jagath J. Kaluarachchi[2]

1 Minnesota Department of Natural Resources, Minnesota, USA

2 Utah State University, Logan, Utah, USA

*Address all correspondence to: kimhomin83@gmail.com

References

[1] Penman HL. Natural evaporation from open water, bare and grass. Proceedings of the Royal Society A: Mathematical, Physical and Engineering Sciences. 1948;**193**(1032):120-145

[2] Allen RG, Pereira LS, Raes D, Smith M. Crop evapotranspiration: Guidelines for computing crop water requirements. In: FAO Irrigation and Drainage Papers, Paper No. 56. Rome: Food and Agriculture Organization of the United Nations; 1998

[3] Bouchet RJ. Evapotranspiration reelle et potentielle, signification climatique [Actual and potential evapotranspiration climate service]. International Association of Scientific Hydrology. 1963;**62**:134-142. France

[4] Granger RJ, Gray DM. Evaporation from natural non-saturated surface. Journal of Hydrology. 1989;**111**:21-29

[5] Anayah FM, Kaluarachchi JJ. Improving the complementary methods to estimate evapotranspiration under diverse climatic and physical conditions. Hydrology and Earth System Sciences. 2014;**18**:2049-2064

[6] Priestley CHB, Taylor RJ. On the assessment of surface heat fluxes and evaporation using large-scale parameters. Monthly Weather Review. 1972;**100**:81-92

[7] Hobbins MT, Ramirez JA, Brown TC, Classens LHJM. The complementary relationship in estimation of regional evapotranspiration: The complementary relationship areal evapotranspiration and advection-aridity models. Water Resources Research. 2001;**37**(5):1367-1387

[8] Fu BP. On the calculation of the evaporation from land surface (in Chinese). Scientia Atmospherica Sinica. 1981;**5**(1):23-31

[9] Yang D, Sun F, Liu Z, Cong Z, Lei Z. Interpreting the complementary relationship in non-humid environments based on the Budyko and Penman hypotheses. Geophysical Research Letters. 2006;**33**:L18402

[10] Zhang L, Hickel K, Dawes WR, Chiew FHS, Western AW, Briggs PR. A rational function approach for estimating mean annual evapotranspiration. Water Resources Research. 2004;**40**:02502

[11] Li D, Pan M, Cong Z, Zhang L, Wood E. Vegetation control on water and energy balance within the Budyko framework. Water Resources Research. 2013;**49**:969-976

[12] Morton FI. Operational estimates of areal evapotranspiration and their significance to the science and practice of hydrology. Journal of Hydrology. 1983;**66**:1-76

[13] Barrow CJ. In: Middleton N, Thomas DSG, editors. World Atlas of Desertification (United Nations Environment Programme). London: Edward Arnold; 1992

[14] Xu CY, Singh VP. Evaluation of three complementary relationship evapotranspiration models by water balance approach to estimate actual regional evapotranspiration in different climate regions. Journal of Hydrology. 2005;**308**:105-121. ISSN: 0022-1694

[15] Kim H, Kaluarachchi JJ. Estimating evapotranspiration using the complementary relationship and the Budyko framework. Journal of Water and Climate Change. 2017;**8**(4):771-790. DOI: 10.2166/wcc.2017.148

[16] Senay GB, Bohms S, Singh RK, Gowda PH, Velpuri NM, Alemu H, et al. Operational

evapotranspiration mapping using remote sensing and weather datasets: A new parameterization for the SSEB approach. Journal of the American Water Resources Association. 2013;**49**:577-591

[17] Aminzadeh M, Roderick ML, Or D. A generalized complementary relationship between actual and potential evaporation defined by a reference surface temperature. Water Resources Research. 2016;**52**:385-406

[18] Kahler DM, Brutsaert W. Complementary relationship between daily evaporation in the environment and pan evaporation. Water Resources Research. 2006;**42**:W05413

[19] Kim D, Rhee J. A drought index based on actual evapotranspiration from the Bouchet hypothesis. Geophysical Research Letters. 2016;**43**:10277-10285

[20] Abramowitz M, Stegun IA. Handbook of Mathematical Functions, with Formulas, Graphs, and Mathematical Tables. Washington D.C, USA: Dover Publications; 1965. 1046p

[21] Farahmand A, AghaKouchak A. A generalized framework for deriving nonparametric standardized indicators. Advances in Water Resources. 2015;**76**:140-145

[22] Vicento-Serrano SM, Begueria S, Lopez-Moreno JI. A multiscalar drought index sensitive to global warming: The Standardized Precipitation Evapotranspiration Index. Journal of Climate. 2010;**23**:1696-1718

[23] Hobbins MT, Wood A, McEvoy DJ, Huntington JL, Morton C, Anderson M, et al. The evaporative demand drought index: Part I- Linking drought evolution to variations in evaporative demand. Journal of Hydrometeorology. 2016;**17**:1745-1761. DOI: 10.1175/jmh-d-15-0121.1

[24] Kim H, Kaluarachchi JJ. Developing an integrated complementary relationship for estimating evapotranspiration. Natural Resources. 2018;**9**:89-109. DOI: 10.4236/nr.2018.94007

[25] Allen RG, Tasumi M, Morse A, Trezza R. Satellite-based energy balance for mapping evapotranspiration with internalized calibration (METRIC): Model. Journal of Irrigation and Drainage Engineering. 2007;**133**(4):380-394

[26] Svoboda M, LeComte D, Hayes M, Heim R, Gleason K, Angel J, et al. The drought monitor. Bulletin of the American Meteorological Society. 2002;**83**:1181-1190

[27] Guo Z, Dirmeyer PA, Koster RD, Bonan G, Chan E, Cox P, et al. GLACE: The global land-atmosphere coupling experiment. Part II: Analysis. Journal of Hydrometeorology. 2006;**7**:611-625